Analysis of cross-functionality within LanBTC synthetase complexes from different bacterial sources with respect to production of fully modified lanthipeptides

Chen, Jingqi; Kuipers, Oscar P

Published in:
Applied and environmental microbiology

DOI:
10.1128/AEM.01618-21

AMERICAN SOCIETY FOR MICROBIOLOGY | Applied and Environmental Microbiology®

GENETICS AND MOLECULAR BIOLOGY

Analysis of Cross-Functionality within LanBTC Synthetase Complexes from Different Bacterial Sources with Respect to Production of Fully Modified Lanthipeptides

Jingqi Chen,[a] **Oscar P. Kuipers**[a]

[a]Department of Molecular Genetics, Groningen Biomolecular Sciences and Biotechnology Institute, University of Groningen, Groningen, the Netherlands

ABSTRACT Lanthipeptides belong to a family of ribosomally synthesized and posttranslationally modified peptides (RiPPs) containing (methyl)lanthionine residues. Commonly, class I lanthipeptides are synthesized by a gene cluster encoding a precursor peptide (LanA), biosynthetic machinery (LanBTC), a protease (LanP), a two-component regulatory system (LanRK), and an immunity system (LanI and LanFEG). Although nisin and subtilin are highly similar class I lanthipeptides, the cross-regulation by LanRK and the cross-immunity by LanI and LanFEG between the nisin and subtilin systems have been proven to be very low. Here, the possibility of the cross-functionality of LanBTC to modify and transport nisin precursor (NisA) and subtilin precursor (SpaS) was evaluated in *Bacillus subtilis* and *Lactococcus lactis*. Interestingly, we found that a promiscuous NisBC-SpaT complex is able to synthesize and export nisin precursor, as efficiently as the native nisin biosynthetic machinery NisBTC, in *L. lactis* but not *B. subtilis*. The assembly of the NisBC-SpaT complex at a single microdomain, close to the old cell pole, was observed by fluorescence microscopy in *L. lactis*. In contrast, such a complex was not formed in *B. subtilis*. Furthermore, the isolation of the NisBC-SpaT complex and its subcomplexes from the cytoplasmic membrane of *L. lactis* by pulldown assays was successfully conducted. Our work demonstrates that the association of LanBC with LanT is critical for the efficient biosynthesis and secretion of the lanthipeptide precursor with complete modifications and suggests a cooperative mechanism between LanBC and LanT in the modification and transport processes.

IMPORTANCE A multimeric synthetase LanBTC complex has been proposed for the *in vivo* production of class I lanthipeptides. However, it has been demonstrated that LanB, LanC, and LanT can perform their functionality *in vivo* and *in vitro*, independently of other Lan proteins. The role of protein-protein interactions, especially between the modification complex LanBC and the transport system LanT, in the biosynthesis process of lanthipeptides is still unclear. In this study, the importance of the presence of a well-installed LanBTC complex in the cell membrane for lanthipeptide biosynthesis and transport was reinforced. In *L. lactis*, the recruitment of SpaT from the peripheral cell membrane to the cell poles by the NisBC complex was observed, which may explain the mechanism by which the secretion of the premature peptide is prevented.

KEYWORDS lanthipeptides, nisin, subtilin, cross-functionality, LanBTC complex, ABC transporter

Lanthipeptides form a large group of ribosomally synthesized and posttranslationally modified peptides (RiPPs) containing (methyl)lanthionine residues (1, 2). According to the posttranslational modification (PTM) enzymes that carry out (methyl)lanthionine ring formation, lanthipeptides are mainly subdivided into four classes (I to IV). Recently, a new class of lanthipeptides (class V) was designated as a result of the discovery of a

Editor Johanna Björkroth, University of Helsinki

Address correspondence to Oscar P. Kuipers, o.p.kuipers@rug.nl.

The authors declare no conflict of interest.

Received 12 August 2021
Accepted 3 November 2021
Accepted manuscript posted online 17 November 2021
Published 25 January 2022

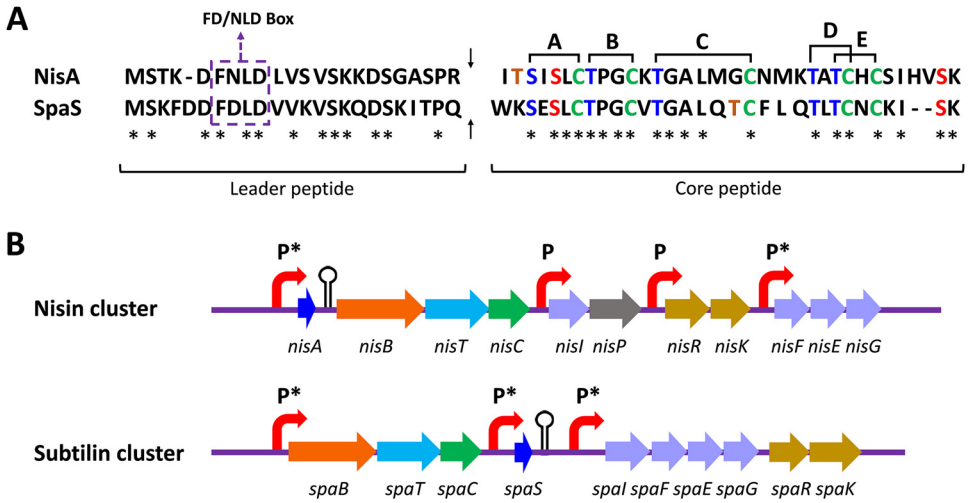

FIG 1 Nisin and subtilin systems and their biosynthetic gene clusters. (A) Comparative analysis of nisin precursor (NisA) and subtilin precursor (SpaS). The conserved FD/NLD box in the leader peptide is highlighted by the purple box. A to E represent different thioether rings. Ser and Thr residues that are involved in ring formation are shown in blue. Ser and Thr residues that are dehydrated but not involved in ring formation are shown in red and yellow. Cys residues that are involved in ring formation are indicated in green. *, identical amino acid residues in NisA and SpaS. The arrows indicate the cleavage site by proteases. (B) The biosynthetic gene clusters of nisin (from *L. lactis* NZ9700) (3) and subtilin (from *B. subtilis* ATCC 6633) (14), encoding precursor peptide (NisA/SpaS), modification enzymes (NisBC/SpaBC), a transporter (NisT/SpaT), a protease (NisP), a two-component regulation system (NisRK/SpaRK), and an immunity system (NisI, NisFEG/SpaI, and SpaFEG). The promoters indicated by P* are activated by mature nisin or subtilin. Other promoters (P) are constitutive.

lexapeptide (2). Lanthipeptides with antimicrobial activity are called lantibiotics, among which two class I lanthipeptides, i.e., nisin and subtilin, are the most thoroughly studied examples (3). Nisin and subtilin exhibit identical topologies of lanthionine ring structures and differ in primary sequence by 14 amino acids (41% difference). Their leader peptides share high amino acid sequence identity, and both contain a conserved FN/DLD motif, which is crucial for recognition by the modification enzymes and transporter (Fig. 1A). The nisin producer *Lactococcus lactis* and the subtilin producer *Bacillus subtilis* ATCC 6633 have similar compositions of genes within the lanthipeptide biosynthetic gene cluster (4, 5) (Fig. 1B). *lanA* is the structural gene of lanthipeptide precursor (6). The genes *lanBTC* encode two modification enzymes and a homodimeric ATP-binding cassette (ABC) transporter (7, 8). The genes *lanRK* code for a two-component system consisting of a histidine kinase and a response regulator (9). The genes *lanI* and *lanFEG* encode a self-immunity system composed of an immunity lipoprotein and an ABC transporter (10). *lanP* is the structural gene for a serine protease, which exists in the nisin system but is deficient in the subtilin system, where its role is performed by some general proteases, i.e., AprE, WprA, Vpr, and Bpr (11, 12).

In the 1990s, the presence of a membrane-associated multimeric LanBTC synthetase complex, such as NisBTC in *L. lactis* (13) and SpaBTC in *B. subtilis* (14), was proposed for the biosynthesis of class I lanthipeptides. This complex catalyzes the dehydration of serine and threonine residues (LanB) and the nucleophilic intramolecular addition of C-terminal cysteine residues with the corresponding dehydrated amino acids (LanC) in the core peptide, followed by transport through the cytoplasmic membrane (LanT). Khusainov et al. demonstrated the copurification of the nisin modification enzymes NisB and NisC with an engineered nisin precursor by a pulldown assay (15). Reiners et al. performed the assembly of the modification machinery NisABC *in vitro* and determined the stoichiometry of the NisABC complex (16). In 2020, the subcellular localization and assembly process of the NisBTC complex for nisin biosynthesis were elucidated in *L. lactis* by advanced fluorescence microscopy. A model wherein nisin precursor is synthesized and secreted mainly at the old cell poles was described (17). Very recently, a heterologous expression system for

nisin was established in *B. subtilis*, and the detailed assembly dynamics of NisBTC were probed in rod-shaped cells by a strategy of timed expression (18). Furthermore, the intact NisBTC complex was isolated from the cell membranes of both *L. lactis* (19) and *B. subtilis* (18). A combined *in vivo* and *in vitro* study characterized the impact of the nisin modification enzymes on the transport kinetics of NisT and suggested a pivotal role of NisB for NisT in the secretion process (20). Overall, these studies emphasize the importance of an intact LanBTC complex for the efficient production and secretion of lanthipeptides, while LanB, LanC, and LanT are capable of performing their respective functionalities independently (8, 21, 22).

The cross-functionality between the nisin and subtilin systems has been intensively studied, inspired by their high similarity (see Table S1 in the supplemental material). The leader peptide of subtilin has been shown to direct the modification and secretion of nisin Z precursor in *L. lactis* (23). The biosynthesis of a few nisin-subtilin chimeras has been assessed in *B. subtilis* (24). Nisin is the activator of the NisRK two-component system but cannot activate the SpaRK system. Subtilin can activate histidine kinase SpaK but cannot activate NisK (25, 26). However, when the N-terminal tryptophan of subtilin is singly changed to an aliphatic amino acid residue, i.e., isoleucine, leucine, or valine, NisK could be activated. Subtilin-nisin hybrids that are able to activate both the SpaK and NisK histidine kinases can also be generated (25). The nisin immunity proteins NisI and NisFEG are specific to nisin and provide no tolerance to subtilin. They are able to protect the heterologous host *B. subtilis* against nisin after coordinated expression (27). Similarly, the lipoprotein SpaI confers immunity against only subtilin (28). The serine protease NisP can release active nisin from the nisin leader peptide but is unable to recognize the subtilin leader (29). Apart from the studies mentioned above, information about cross-modification by LanBC and cross-transport by LanT between different lanthipeptide systems is scarce.

Here, we describe an *in vivo* study of the interfunctionality of the subtilin transporter SpaT in *L. lactis* and the subcellular localization of the NisBC-SpaT complex formed. SpaBC is unable to recognize and modify the NisA peptide, whereas SpaT can export the nisin precursor that has been fully modified, as efficiently as the native transporter NisT, in *L. lactis*. By advanced fluorescence microscopy, two distinct assembly situations of the potential LanBTC complex were revealed in *L. lactis* and *B. subtilis*. In agreement with this, the promiscuous NisBC-SpaT complex was isolated from the cytoplasmic membrane of *L. lactis*. Our data reinforce the subcellular distribution of the LanBTC machinery at the old cell poles in coccoid cells and imply an indispensable cooperative manner of such a complex functioning during lanthipeptide biosynthesis.

RESULTS

A nisin precursor with incomplete modification is exported by the subtilin transporter SpaT in *B. subtilis*. Although a heterologous production and secretion platform for fully modified nisin precursor was established in *B. subtilis* recently (18), the yield of the exported peptide by the dedicated ABC transporter NisT was low in comparison with its secretion by the native producing strain of *L. lactis*. It has been demonstrated that a few posttranslationally dehydrated peptides and a thioether-bridged azurin peptide fragment could be transported via the Sec pathway in *L. lactis* (30, 31). In our initial attempt, five widely used *B. subtilis* signal peptides, including three Sec signal peptides, SP_{AmyE} (32), SP_{AprE} (33), and SP_{Epr} (34), and two Tat signal peptides, SP_{PhoD} (35) and SP_{YwbN} (36), were each fused to the N terminus of NisA. The fusion peptides were coexpressed with NisB and NisC in *B. subtilis* WB800. However, no fusion peptide was detected in the culture supernatant by SDS-PAGE and Western blotting, while all peptides were expressed in the cells (Fig. 2A). This demonstrates that in *B. subtilis*, the Sec machinery and Tat machinery are unsuitable to be used to transport NisA even when the leader peptide is preceded by a signal peptide.

Subtilin, a lanthipeptide highly similar to nisin, is a natural product exported by the ABC transporter SpaT in *B. subtilis* ATCC 6633 (29, 37). It has been reported that the leader peptide of SpaS could direct the secretion of nisin through the NisT transport system in *L.*

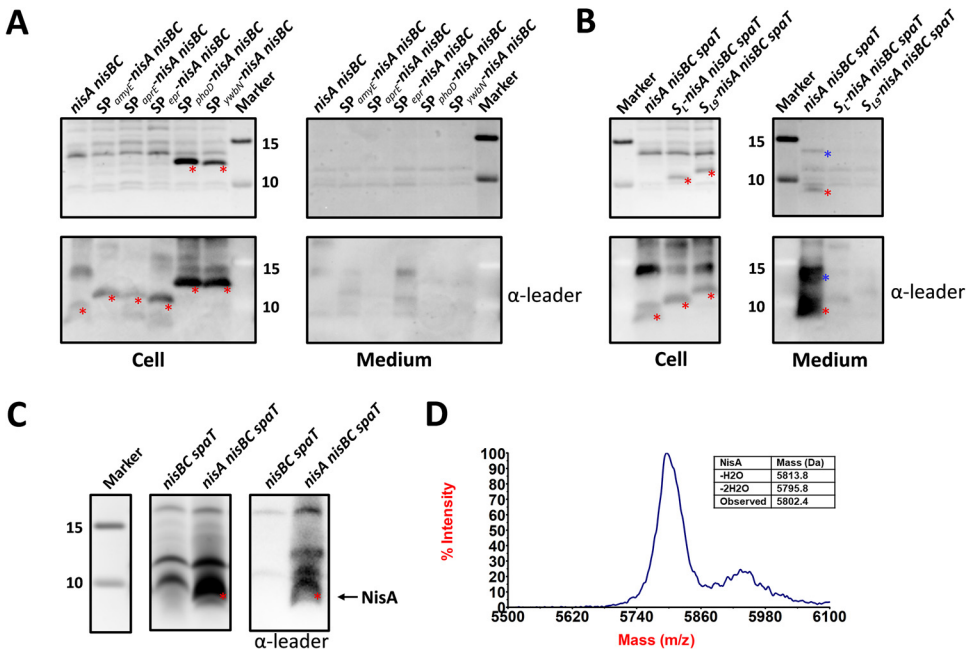

FIG 2 Production of nisin precursor in *B. subtilis* WB800. (A) Evaluation of the use of Sec and Tat signal peptides to direct the secretion of NisA by SDS-PAGE (top lane) and Western blotting using antileader antibody (bottom lane). Three Sec signal peptides (SP_{AmyE}, SP_{AprE}, and SP_{Epr}) and two Tat signal peptides (SP_{PhoD} and SP_{YwbN}) were fused to the N terminus of NisA. WB800 *thrC*::P_{xylA}-*nisBC*/pKTH11-*nisA* was used as a control. (B) Secretion of the NisA peptide and the engineered NisA peptide with a partial SpaS sequence, mediated by SpaT. S_L-*nisA*, the leader peptide of SpaS (S_L), was fused to the N terminus of NisA. S_{L9}-*nisA*, the leader peptide of SpaS plus 9 N-terminal core peptide residues (S_{L9}), was fused to the N terminus of NisA. SDS-PAGE analysis is shown in the top lane. Western blot analysis is shown in the bottom lane. (C) Detection of TCA-precipitated NisA from the culture supernatant. SDS-PAGE analysis is shown in the middle lane. Western blot analysis is shown in the right lane. The red asterisks in panels A to C indicate the corresponding peptides in the cell or medium. The blue asterisks in panel B show dimeric NisA. (D) MALDI-TOF MS data for TCA-precipitated NisA. The sample is the same as that in panel C.

lactis (23, 38). Inspired by this, we wondered whether SpaT is able to recognize the NisA leader peptide and thus export NisA to the exterior. The structural gene *spaT* under the control of an isopropyl β-D-1-thiogalactopyranoside (IPTG)-inducible hyperspank promoter (P_{hy_spank}) was introduced in the *amyE* locus of the chromosome in *B. subtilis* that produces NisA, NisB, and NisC. In the supernatant of the cell culture, two bands corresponding to monomeric NisA (6.0 kDa) and dimeric NisA (12.0 kDa) were observed by SDS-PAGE and Western blot analysis using antileader antibody (Fig. 2B). The supernatant was precipitated by the use of trichloroacetic acid (TCA) (Fig. 2C). Matrix-assisted laser desorption ionization–time of flight mass spectrometry (MALDI-TOF MS) analysis of the concentrated peptide showed that the secreted peptide was dehydrated only once or twice (Fig. 2D). To determine the modification state of the intracellular peptide, NisA was C-terminally extended with a factor Xa sequence, a flexible linker, and a 6×His tag, termed $NisA_{GS\text{-}His}$ (see Fig. S1A in the supplemental material). Affinity-purified $NisA_{GS\text{-}His}$ was eluted with a good yield and was found to be dehydrated five times out of eight possible dehydrations (Fig. S1B and C). When the leader peptide of SpaS (S_L) or S_L with the N-terminal 9 residues of the SpaS core peptide (S_{L9}) was fused to the N terminus of NisA, unexpectedly, almost no peptide was detected in the culture supernatant, while cellular peptide accumulation was observed (Fig. 2B). According to these data, we conclude that SpaT possesses the ability to transport NisA. However, it appears that the secretion of NisA occurs here prior to its modification in *B. subtilis*.

Fully modified nisin precursor is transported by the subtilin transporter SpaT, as efficiently as by the native transporter NisT, in *L. lactis*. Since *L. lactis* is the native producing strain for nisin, it is interesting to assess the transport ability of SpaT for nisin precursor in *L. lactis*. The gene *nisT* was deleted from the wild-type operon *nisABTC*

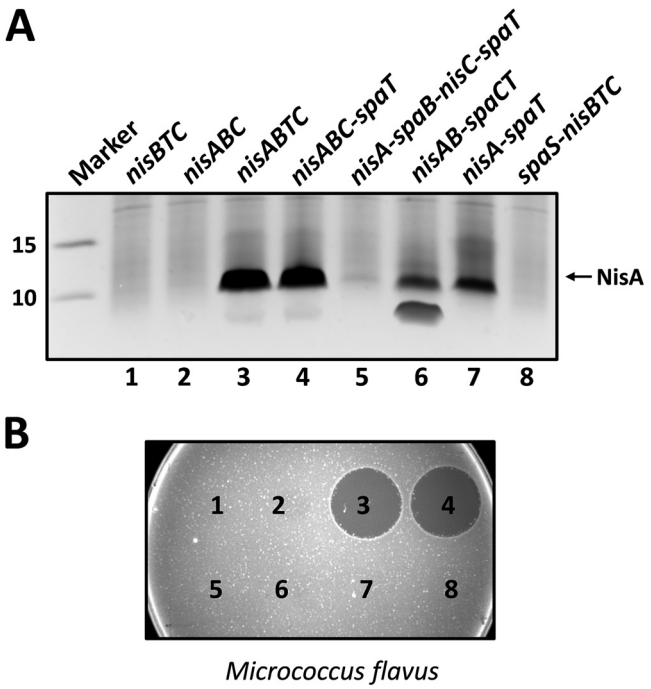

FIG 3 Secretion of NisA mediated by SpaT in *L. lactis*. (A) SDS-PAGE analysis of NisA in the culture supernatant. The supernatant was TCA precipitated prior to SDS-PAGE. (B) Antimicrobial activity of NisA from the supernatant of the cell culture. The supernatant was incubated with the purified protease NisP to remove the leader peptide from NisA, releasing the core peptide. *Micrococcus flavus* was used as the indicator strain. The same numbers in panels A and B represent the same samples, respectively.

that is located in the multicopy expression plasmid pTLR4-*nisABTC*, while the gene *spaT* was inserted downstream of the resulting operon *nisABC*, generating a new gene cluster, *nisABC-spaT*, which is regulated by the nisin-inducible promoter (P_{nisA}). Prior to SDS-PAGE, the culture supernatant was concentrated by TCA precipitation. We not only found that the nisin precursor was exported by SpaT but also observed that the secretion level of the peptide was relatively high, comparable to its secretion mediated by NisT (Fig. 3A). Peptides from both concentrated supernatants exhibited identical antimicrobial activities (Fig. 3B). Furthermore, the secreted peptides were purified by C_{18} reversed-phase chromatography. MALDI-TOF MS showed that in both cases, the peptides had been dehydrated eight times (Fig. 4A). These results demonstrate that SpaT is capable of transporting nisin precursor as efficiently as NisT. Notably, all the secreted peptide had been fully modified by NisBC before being transported by SpaT, consistent with the mechanism by which the export of premature peptide is prevented when the transporter is NisT. In contrast, when *nisB* or *nisC* in the operon *nisABC-spaT* was replaced by *spaB* or *spaC*, correspondingly, the secretion efficiency of nisin precursor was severely decreased, particularly in the former situation (Fig. 3A). For both enzyme combinations (SpaB-NisC and NisB-SpaC), the antimicrobial activity of the TCA-precipitated supernatant was not observed (Fig. 3B). In the case of SpaB-NisC, the secreted peptide was not dehydrated at all (Fig. 4A), which implies that SpaB could not catalyze the dehydration reaction in the NisA core peptide. When NisB and SpaC were combined to be expressed, the exported peptide was dehydrated eight times (Fig. 4A). Two thioether rings were likely formed since 3 free cysteine residues were detected by a CDAP (1-cyano-4-dimethylaminopyridinium tetrafluoroborate) coupling assay (Fig. 4B). These results suggest that SpaC was unable to perform the full cyclization reactions in the core peptide, although the peptide had been completely dehydrated by NisB. When NisA was coexpressed with only SpaT, no dehydration and cyclization took place in the core peptide of NisA (Fig. 3B and Fig. 4B). The secretion level was low,

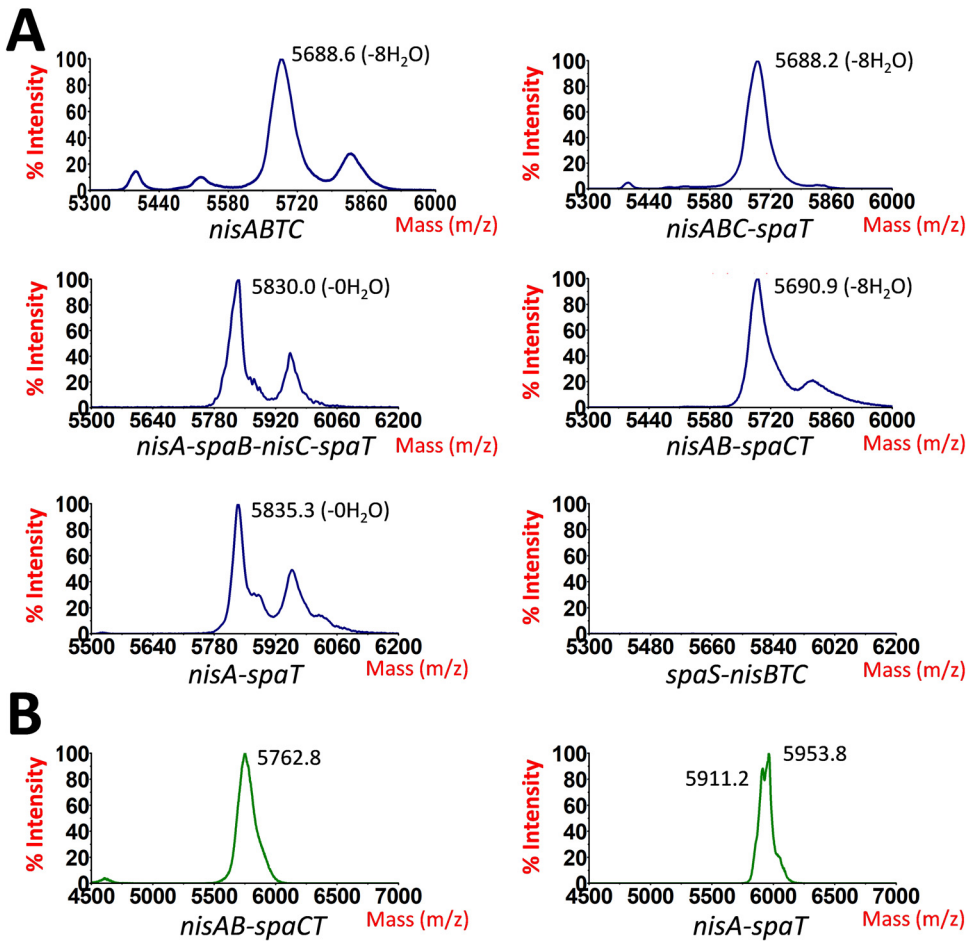

FIG 4 Determination of the numbers of dehydration and cyclization reactions in nisin precursor. (A) MALDI-TOF MS analysis of the peptides secreted by *L. lactis*. The calculated mass of NisA with eight dehydrations is 5,687.8 Da. The calculated mass of NisA with no dehydration is 5,831.8 Da. (B) MALDI-TOF MS analysis of the exported peptides with CDAP coupling. When a cysteine residue is not part of a thioether ring, the free thiol group of the cysteine residue can be cyanilated with CDAP, and a mass shift of 25 Da can be observed. In the left lane, a mass shift of 75 Da (from 5,687.8 to 5,762.8 Da) was observed, demonstrating that 2 cysteine residues were coupled and that 3 were free in the peptide. In the right lane, a mass shift of 122 Da (from 5,831.8 to 5,953.8 Da) was observed, showing 5 free cysteine residues in the unmodified peptide. In panels A and B, the peptides used were purified by C_{18} reversed-phase chromatography.

while it was much higher in the situation where both NisB and NisC were present. Based on all the above-described data, we conclude that the dedicated subtilin transporter SpaT transports nisin precursor after complete modification by NisBC occurs in *L. lactis*. This suggests a cooperative mechanism between SpaT and NisBC, as observed between NisT and NisBC. However, as for subtilin modification enzymes, neither SpaB nor SpaC is available to be used to correctly modify the NisA peptide, probably due to its failure to recognize the leader peptide of this heterologous substrate. Similarly, the subtilin precursor SpaS could not be modified and transported by the nisin biosynthetic machinery NisBTC in *L. lactis*, as we observed (Fig. 3).

The nisin modification machinery NisBC and the subtilin transporter SpaT do not fully assemble as a complex in *B. subtilis*. We have demonstrated the actual transport of nisin precursor by SpaT in both *B. subtilis* and *L. lactis*. Although completely modified NisA was produced by the *L. lactis* system, the peptide secreted by *B. subtilis* was proven to be modified with a very limited number of dehydrations. What is the reason for this difference despite the use of the same enzymes and transporter? Since several studies have suggested that a multimeric lanthionine synthetase complex is present at the cytoplasmic membrane for the production of lanthipeptides (17, 20,

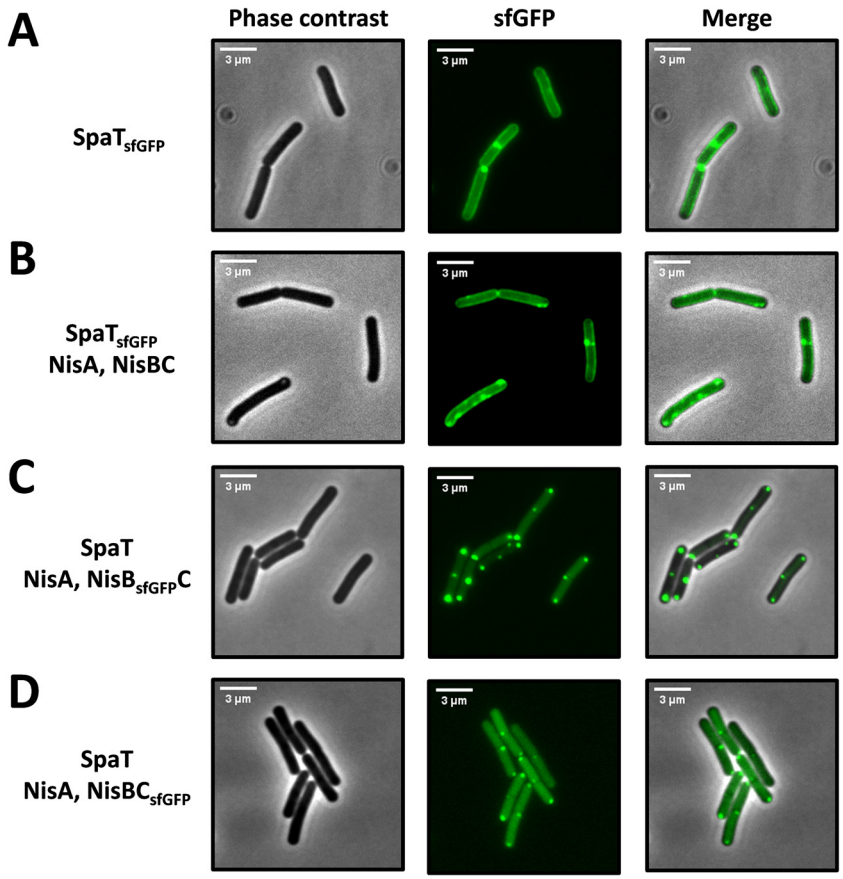

FIG 5 Determination of the subcellular localization of SpaT, NisB, and NisC in *B. subtilis* WB800 by advanced fluorescence microscopy. (A) SpaT$_{sfGFP}$ was expressed alone in WB800. (B) SpaT$_{sfGFP}$ was coexpressed with NisA, NisB, and NisC. (C) NisB$_{sfGFP}$ was expressed in the presence of NisA, NisC, and SpaT. (D) NisC$_{sfGFP}$ was expressed in the presence of NisA, NisB, and SpaT.

39), we hypothesized that such a functional complex might not be available in *B. subtilis* when SpaT is coexpressed with NisABC. To address this question, the subcellular distribution of NisB, NisC, and SpaT was determined by fluorescence microscopy. Superfolder green fluorescent protein (sfGFP) was used to label SpaT at its C terminus, generating the fusion protein SpaT$_{sfGFP}$. When SpaT$_{sfGFP}$ was expressed alone in *B. subtilis* WB800, SpaT$_{sfGFP}$ circumferentially distributed throughout the cytoplasmic membrane was observed, with rare bright foci only at some of the cell poles or the septum (Fig. 5A). After the introduction of the expression of NisA, NisB, and NisC, no significant variation in SpaT$_{sfGFP}$ localization was found (Fig. 5B). When NisB or NisC was C-terminally labeled by sfGFP but SpaT was kept tag free, we found that both enzymes were mainly localized at the cell poles and septum, functioning as modification machinery (Fig. 5C and D). The different localizations of NisBC and SpaT suggest that a promiscuous nisin biosynthetic machinery was not assembled, at least not fully formed at the cytoplasmic membrane. The hypothesis proposed above was therefore verified by this experimental result. It is tempting to speculate that the affinity of SpaT for NisBC is insufficient to recruit NisBC to the discrete secretion site to assemble a functional LanBTC complex, although this recruitment process during NisBTC formation has been described in *B. subtilis* (18).

Diffuse SpaT throughout the membrane is recruited to the old cell poles by NisBC, generating functional promiscuous machinery for nisin biosynthesis in *L. lactis*. In our previous study, when NisA, NisB, NisC, and mutant NisT were expressed in *L. lactis*, the nisin biosynthetic machinery NisBTC was found to be assembled at the old cell poles (17). The question of whether a LanBTC complex is formed in *L. lactis* cells

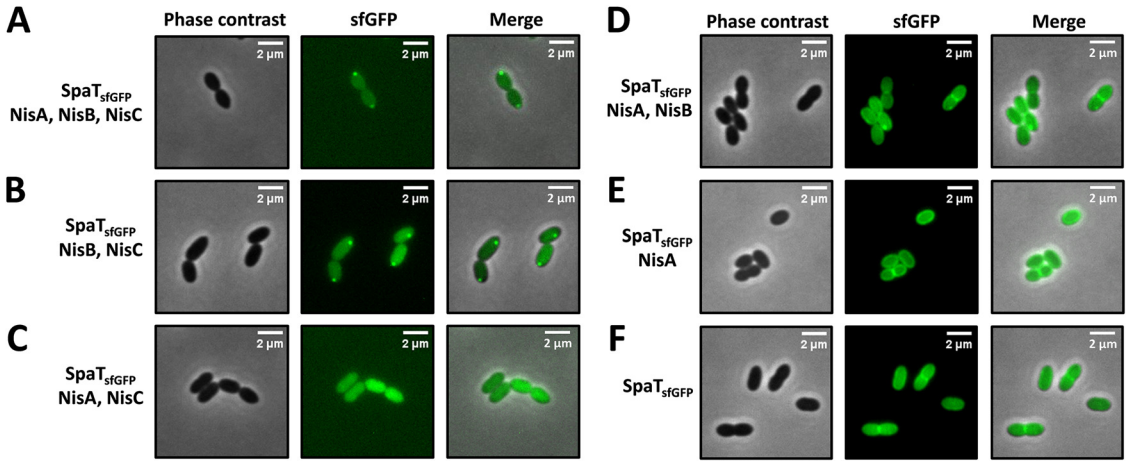

FIG 6 Determination of the subcellular localization of SpaT in *L. lactis* NZ9000 carrying different gene combinations. (A) NZ9000/pTLR4-*nisABC-spaT*$_{sfgfp}$. (B) pTLR4-*nisBC-spaT*$_{sfgfp}$. (C) pTLR4-*nisAC-spaT*$_{sfgfp}$. (D) pTLR4-*nisAB-spaT*$_{sfgfp}$. (E) pTLR4-*nisA-spaT*$_{sfgfp}$. (F) pTLR4-*spaT*$_{sfgfp}$. In panels A to F, SpaT was labeled by sfGFP at its C terminus.

when SpaT and NisABC are coexpressed remained to be answered. For this purpose, fluorescence microscopy was employed to determine the subcellular distribution of SpaT and NisBC. In the presence of NisABC, the fusion protein SpaT$_{sfGFP}$ was found to be dominantly confined to the cell poles (Fig. 6A). In the same system, when NisC was N-terminally tagged by mCherry (red fluorescence protein), we observed that the clusters of SpaT$_{sfGFP}$ and $_{mCherry}$NisC were always colocalized at the regions of the cell poles according to the merged images (Fig. 7A), which was also supported by the quantitative colocalization analysis (Pearson's correlation coefficient [PCC] $r = 0.96$) (Fig. 7B). As fluorescently labeled NisC-associated foci represent the NisABC complex, and the cell poles where NisABC is located have been shown to be the old ones (17), we conclude that the bright foci were the promiscuous NisBC-SpaT complex, and they were localized at the old cell poles. Here, the visualization of NisBC-SpaT foci was performed in a situation where the SpaT transport system was highly active, whereas the previously revealed NisBTC foci could be probed only when nisin secretion was blocked.

To characterize the interactions of SpaT with NisA, NisB, and NisC, various expression combinations were created. When NisA was deficient, the polar localization was maintained for SpaT$_{sfGFP}$ (Fig. 6B). This demonstrates that the assembly of NisBC-SpaT is not substrate dependent. In the absence of NisB, NisT$_{sfGFP}$ was not localized at the cell poles anymore but became totally diffuse throughout the cells (Fig. 6C). The lack of NisC led to a circumferential distribution of SpaT$_{sfGFP}$ across the cytoplasmic membrane, with only occasional enhanced bright foci close to the cell poles (Fig. 6D). In cells where both NisB and NisC were deficient but NisA was expressed, the fluorescence signal of SpaT$_{sfGFP}$ clearly displayed a uniform distribution throughout the cell membrane, without any enhanced bright foci (Fig. 6E). A similar subcellular localization was observed when SpaT$_{sfGFP}$ was expressed alone (Fig. 6F). Altogether, a recruitment behavior of SpaT by NisBC from the cell membrane to the old cell poles is proposed based on these observations, as we previously observed for NisT in *L. lactis* (17). We noticed that NisB alone is unable to totally target SpaT to the pole regions, although its expression resulted in a polar localization for SpaT in some cells. Besides NisB, NisC is also required for the full recruitment of SpaT. Therefore, it is likely that NisC assists in the movement of SpaT to the cell poles promoted by NisB. Here, we can observe a cooperative action for NisB and NisC in the assembly of the LanBTC complex.

Isolation of the promiscuous NisBC-SpaT complex and its subcomplexes from the cytoplasmic membrane of *L. lactis* cells. Recently, the intact nisin biosynthetic machinery NisBTC was successfully isolated from the cytoplasmic membranes of both *L. lactis* and *B. subtilis* by using the strategy of pulldown (18, 19). We attempted to isolate the NisBC-SpaT complex that was visualized as described above in *L. lactis* cells in

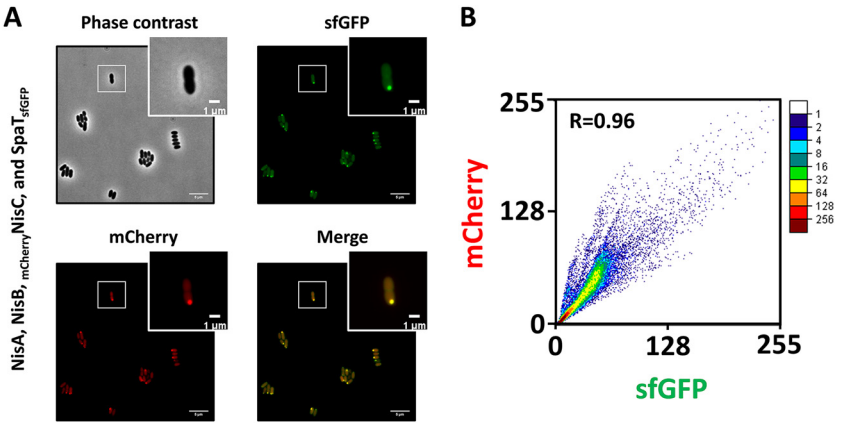

FIG 7 Colocalization of SpaT with the nisin modification machinery NisBC in *L. lactis*. (A) SpaT$_{sfGFP}$ and $_{mCherry}$NisC were mainly colocalized at the old cell poles in the presence of NisA and NisB. The localization of $_{mCherry}$NisC represents the distribution of NisBC. (B) Colocalization analysis of the clusters of SpaT$_{sfGFP}$ and $_{mCherry}$NisC. Pearson's correlation coefficients (PCCs) (*R*) between the green foci and red foci are shown in a scatter diagram on the right. The PCCs range from +1 (perfect correlation) to −1 (perfect but negative correlation), with 0 denoting the absence of a relationship.

the same way. The peptide and proteins were overexpressed in *L. lactis* NZ9000 carrying two multicopy expression plasmids: pNZE3-*nisA-spaT*$_{His}$, harboring the genes encoding tag-free NisA and SpaT that is labeled by a 6×His tag at its C terminus, and pIL3-*nisB*$_{flag}$*C*, expressing C-terminally Flag-tagged NisB and tag-free NisC. All four genes were regulated by the nisin-inducible promoter P$_{nisA}$ (40). The cytoplasmic membrane was separated, solubilized in the mild detergent *n*-dodecyl-β-D-maltoside (DDM), and applied for affinity purification by Ni-nitrilotriacetic acid (NTA) chromatography. SpaT$_{His}$ was found to be purified with a migrated band smaller than the calculated size (72.3 kDa), showing higher mobility, similar to NisT (18) and other membrane proteins (Fig. 8A and B). Western blot analysis indicated that both NisB$_{Flag}$ (120.2 kDa) and NisC (47.9 kDa) were eluted together with SpaT$_{His}$ (Fig. 8C and D). The substrate NisA was not detected in the same eluate by Western blotting, probably due to its weak affinity for SpaT and the low yield of copurification (Fig. S2). Taken together, the pulldown assays demonstrate that the promiscuous but functional NisBC-SpaT complex was isolated from the cell membrane of *L. lactis*.

To gain insight into the detailed interactions between the proteins of this promiscuous complex, isolation of SpaT-associated subcomplexes from a series of *L. lactis* strains was conducted (Fig. 8). When NisA was not available for the enzymes and transporter, the purification of SpaT$_{His}$ still pulled down both NisB$_{Flag}$ and NisC. This indicates that NisBC-SpaT formation does not need the trigger by the substrate peptide, in line with the visualization of NisBC-SpaT foci at the old cell poles where no NisA was present. When SpaT$_{His}$ was coexpressed with either NisB$_{Flag}$ or NisC, the complexes SpaT-NisB and SpaT-NisC were detected in the eluates, respectively, as revealed by Western blotting. This result demonstrates that SpaT not only interacts with NisB but also associates with NisC, consistent with the finding that NisT directly interacts with both NisB and NisC in *L. lactis* and *B. subtilis* (18, 19). When both enzymes were absent, NisA was found to be copurified with SpaT$_{His}$ (Fig. S2), showing direct binding of LanA to the transporter LanT, although the amount of the coeluted peptide was small. In summary, both NisB and NisC directly interact with SpaT to assemble the NisBC-SpaT complex, which does not need the stimulation of nisin transport through the cell membrane. Although NisT has been purified in abundance using DDM and could be clearly observed by SDS-PAGE, the copurified NisB and NisC were detected only by Western blotting, underlining the relatively weak affinity of both enzymes for the transporter. This is in accordance with the hypothesis that the multimeric lanthionine synthetase complex for nisin biosynthesis is highly unstable and transient (3).

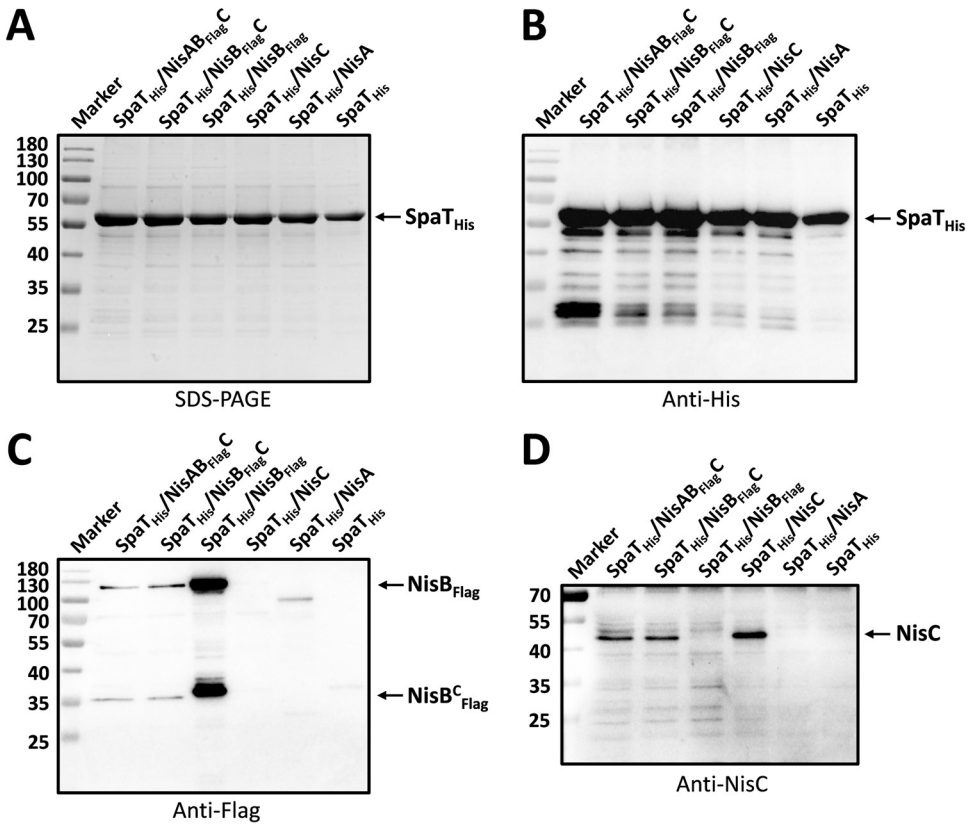

FIG 8 Isolation of the NisBC-SpaT complex and its SpaT-associated subcomplexes. SpaT$_{His}$ was coexpressed with NisA, NisB$_{Flag}$, and NisC in different combinations in *L. lactis* NZ9000. The cell membrane was collected by ultracentrifugation and solubilized using the mild detergent *n*-dodecyl-β-D-maltoside (DDM). The proteins were purified from the solubilized membrane by affinity purification using Ni-NTA agarose. The eluates were analyzed by glycine SDS-PAGE followed by Coomassie G-250 staining and Western blotting using anti-His, anti-Flag, and anti-NisC antibodies, as indicated. SpaT$_{His}$, SpaT C-terminally labeled by a 6×His tag; NisB$_{Flag}$, NisB C-terminally labeled by a Flag tag; NisB$^{C}_{Flag}$, the C-terminal product of degraded NisB labeled by a Flag tag. The size of SpaT$_{His}$ is 72.3 kDa. The size of NisB$_{Flag}$ is 120.2 kDa. The size of NisC is 47.9 kDa.

Interestingly, an ~30-kDa protein (NisB^{C}) was copurified with SpaT$_{His}$ besides full-length NisB in some eluates using anti-Flag antibody (Fig. 8C). A truncated product, the N-terminal ~90-kDa part of NisB, has been reported to be present in the cytoplasm and at the cell membrane of *L. lactis* (15, 41). Hence, we assume that the observed ~30-kDa protein was the C-terminal part of NisB. Since the Flag tag was fused to the C terminus of NisB, the degraded N-terminal part of NisB was not detected but should also be present in the corresponding eluates.

DISCUSSION

LanT is an ABC transporter responsible for the export of class I and II lanthipeptides through the cytoplasmic membrane. In *L. lactis* NZ9700, nisin precursor is transported by the NisT system, while subtilin precursor is exported by the SpaT system in *B. subtilis* ATCC 6633. It has been reported that the leader peptide of subtilin could direct the secretion of nisin through the NisT transport system in *L. lactis* (23, 38). In this study, our results demonstrate that SpaT can export the NisA peptide in the presence of NisB and NisC in *B. subtilis* WB800, although the secreted peptide was not fully modified. The intracellular NisA peptide possesses more dehydrated residues than the extracellular peptide. In *L. lactis*, strikingly, SpaT was able to transport nisin precursor equally as well as its native transporter NisT when both NisB and NisC were coexpressed. Importantly, the secreted peptide had been completely modified and exhibited good antimicrobial activity. Hence, SpaT and NisT display a cross-transport ability with nisin

precursor and subtilin precursor, respectively, although the exported peptide may not always be well modified.

For LanBC, we did not observe the potential ability of SpaB and SpaC to correctly modify NisA since the NisA peptide secreted into the medium was not dehydrated when NisB was replaced by SpaB, and only two lanthionine rings were created when NisC was replaced by SpaC in *L. lactis*. Similarly, the coexpression of SpaS with the nisin biosynthetic machinery NisBTC did not lead to the secretion of either modified or unmodified subtilin precursor. However, after the subtilin leader peptide was fused to the core peptide of NisA, the fusion peptide could be modified by SpaBC and secreted by SpaT in *B. subtilis* (29). Commonly, LanA is composed of an N-terminal leader peptide and a C-terminal core peptide. The well-characterized FNLD box located in the nisin leader peptide is important for the interaction of NisB and NisC with their substrate as well as for peptide secretion mediated by NisT (38, 42, 43). The similar motif in the leader peptide of subtilin is the FDLD box (Fig. 1A). In the situation where the conserved FN/DLD box was altered, it is likely that SpaBC failed to recognize the nisin leader and NisBC could not bind to the subtilin leader, resulting in the unavailability of cross-modification by LanBC. The full functionality of SpaT for both SpaS and NisA indicates that SpaT recognizes not only the sequence FDLD but also FNLD. LanT seems to have a more relaxed substrate specificity than LanBC. This is in line with their similarity: NisT and SpaT have a high sequence identity of 42.4%, while NisBC and SpaBC have relatively low sequence identities of 27.2% and 26.5% (see Table S1 and Fig. S3 in the supplemental material).

In this study, the expression of NisA, NisB, NisC, and SpaT in *B. subtilis* and *L. lactis* resulted in the production of NisA that was in distinct modification states. Although the independent functionalities of NisB, NisC, and NisT have been demonstrated in *in vivo* and *in vitro* ways (8, 21, 22), the presence of the multimeric lanthionine synthetase complex LanBTC and the association of the transporter LanT with the modification complex LanBC have been suggested to be crucial for the efficient biosynthesis of lanthipeptides (13, 14, 17, 20). Since SpaT is a heterologous protein for NisA, NisB, and NisC, we were curious to see whether they could interact with each other and form a functional complex in both systems in the same way as the wild-type machinery NisBTC. In *B. subtilis*, it has been shown that, initially, NisB and NisC assemble as a modification machinery at the cell poles and septum, and subsequently, NisBC is recruited to membrane-located discrete foci by NisT, generating the functional NisBTC complex (18). However, after NisT was replaced by SpaT, the NisBC complex maintained its original localization at the cell poles and septum, while SpaT was uniformly distributed in the cytoplasmic membrane. This implies that the NisBC-SpaT complex was not fully assembled, probably owing to a weak interaction between NisBC and SpaT in *B. subtilis*. It seems that NisA was exported by SpaT prior to being modified by NisBC. In *L. lactis*, the subcellular localization and assembly process of the nisin biosynthetic machinery have been described, and a model for NisBTC assembly mainly at the old cell poles has been proposed (17). Here, NisBTC clusters could be visualized only when nisin secretion was blocked by a point mutation in NisT. Our study shows that in a situation where nisin secretion is highly efficient, SpaT that is originally distributed throughout the membrane could be recruited to the old cell poles by NisBC, forming a promiscuous NisBC-SpaT complex in *L. lactis*. We also found that both NisB and NisC are required for the recruitment process of NisT since single NisB or NisC is unable to attract free SpaT to the export site. Notably, this is new evidence supporting the model where LanBTC assembly and lanthipeptide secretion occur at the old cell poles in coccoid cells. According to the microscopy data, we conclude that the correct assembly of the intact LanBTC complex is necessary for the production and secretion of the fully modified lanthipeptide precursor.

Using the strategy of pulldown, the NisBC-SpaT complex was isolated from the cell membrane, in accordance with the microscopy-visualized formation of the NisBC-SpaT foci. Coupled with the isolation of the wild-type NisBTC complex (18), this provides

direct evidence for the existence of the membrane-associated LanBTC complex for lanthipeptide biosynthesis. Although we purified SpaT in abundance using the detergent DDM, NisB and NisC that copurified with SpaT could be detected only by Western blotting. These results imply a relatively weak affinity of NisBC for SpaT. Certainly, we could not absolutely preclude the influence caused by the different tags introduced into each protein on the protein-protein interactions. The NisBC-SpaT complex is suggested to be highly unstable and transient, similar to the native NisBTC complex. Besides NisBC-SpaT probably carrying NisA, its SpaT-associated subcomplexes, such as NisB-SpaT, NisC-SpaT, and NisBC-SpaT, could also be isolated from the cell membrane. Here, a specific interaction between SpaT and NisC was observed, in agreement with an interaction of NisT with NisC detected previously by coimmunoprecipitation and a yeast two-hybrid assay (13). Moreover, we probed an interaction of SpaT with NisB that was not observed between NisT and NisB in the above-mentioned study but in that case for SpaT and SpaB (14). Our work shows that the substrate peptide is not required for the interaction of SpaT with NisBC. Together with the observations by microscopy, these findings not only imply a role of LanBC as a courier to ship fully modified LanA to LanT for transport beyond the function of modification but also suggest a mechanism by which the premature secretion of unfinished LanA is prevented. LanT is probably inaccessible to unmodified LanA that is dissociated from LanBC since the secretion efficiency of LanT is extremely low when LanBC are deficient. As soon as the modification of LanA by LanBC is finished, the fully modified LanA would be handed over to the transport system LanT, which has been incorporated into the LanBTC machinery via interaction with LanBC, to be exported outside the cells. The *in vitro* assembly of the NisABC complex has been conducted, showing that NisABC is composed of a dimer of NisB, a monomer of NisC, and a NisA monomer (16). However, the exact stoichiometry of the NisABTC complex remains to be elucidated.

In conclusion, we evaluated the potential cross-functionality of LanBTC between the nisin and subtilin systems. LanBC is highly specific for the conserved leader peptide of LanA. However, LanT possesses a relatively relaxed substrate specificity, allowing the employment of LanT to efficiently transport other homologous lanthipeptides, which thus circumvents the need for exchanging the leader peptide, as long as the conserved FN/DLD box is present, which is probably (part of) the recognition site of the transporter. Moreover, two distinct assembly situations for the NisBC-SpaT complex in *B. subtilis* and *L. lactis* reinforce the importance of an intact LanBTC installed at the cytoplasmic membrane for the biosynthesis of fully modified lanthipeptides.

MATERIALS AND METHODS

Bacterial strains and growth conditions. The bacterial strains used in this work are listed in Table 1. *Bacillus subtilis* ATCC 6633 was used as the source of subtilin biosynthetic genes. *Lactococcus lactis* NZ9700 was used as the source of nisin biosynthetic genes. *Micrococcus flavus* was employed as the indicator strain for the detection of fully modified nisin (11). *Escherichia coli* DH5α served as a host for cloning and plasmid preparation. *B. subtilis*, *E. coli*, and *M. flavus* were grown in Luria-Bertani (LB) medium at 37°C under aerobic conditions (with shaking at 220 rpm). *L. lactis* NZ9000 was used as an expression system and was grown as a standing culture at 30°C in Difco M17 medium (BD, Franklin Lakes, NJ, USA) with 0.5% (wt/vol) glucose (GM17) or minimal essential medium (MEM) with 0.5% (wt/vol) glucose. The following antibiotics were added when necessary: 100 μg/mL spectinomycin, 0.5 μg/mL erythromycin, 12.5 μg/mL lincomycin, and/or 25 μg/mL kanamycin for *B. subtilis*; 100 μg/mL ampicillin for *E. coli*; and 5 μg/mL chloramphenicol and/or 5 μg/mL erythromycin for *L. lactis*. For induction in *B. subtilis*, 0.5% (wt/vol) xylose and/or 0.1 mM IPTG was added to the medium to initiate the expression of genes under the control of P_{xylA} and/or P_{hy_spank}. For induction in *L. lactis*, 10 ng/mL nisin Z (Handary SA, Belgium) was added to the medium to initiate the expression of genes under the control of the nisin-inducible promoter P_{nisA}, when the optical density at 600 nm (OD_{600}) of the cell culture reached 0.6. Agar (1.5%, wt/vol) was added to the growth medium as solid medium. All chemicals were purchased from Sigma-Aldrich.

Recombinant DNA techniques and oligonucleotides. Plasmids used and created in this study are listed in Table 1. The techniques for standard molecular cloning were performed as described previously (44). The GenElute genomic DNA kit (Sigma-Aldrich, St. Louis, MO) was used to isolate genomic DNA of *L. lactis*. The NucleoSpin plasmid EasyPure kit (Bioke, Leiden, the Netherlands) and the NucleoSpin gel and PCR cleanup kit (Bioke, Leiden, the Netherlands) were employed to extract plasmids and purify PCR products, respectively, according to the manufacturer's instructions. PCRs were conducted with PrimeSTAR Max DNA polymerase (TaKaRa Bio Europe SAS, Saint-Germain-en-Laye, France) according to

TABLE 1 Strains and plasmids used in this study

Strain or plasmid	Genotype and/or characteristic(s)	Reference or source
Strains		
L. lactis NZ9700	*nisABTCIPRKFEG*; nisin producer	48
B. subtilis ATCC 6633	*spaBTCSIFEGRK*; subtilin producer	14
E. coli DH5α	F$^-$ Δ*lacU169*(ϕ80d *lacZ*ΔM15) *supE44 hsdR17 recA1 gyrA96 endA1 thi-1 relA1*	Lab stock
Micrococcus flavus	Indicator strain for nisin	11
B. subtilis WB800	8-fold protease-deficient strain; Δ*nprE* Δ*nprB* Δ*aprE* Δ*epr* Δ*mpr* Δ*bpr* Δ*vpr* Δ*wprA*	49
L. lactis NZ9000	MG1363 *pepN*::*nisRK*	Lab stock
SC01	WB800 *thrC*::P_{xylA}-*nisBC*; Spec^r	18
SC02	WB800 *thrC*::P_{xylA}-*nisBC*/pKTH11-*nisA*; Spec^r Kan^r	This study
SC03	WB800 *thrC*::P_{xylA}-*nisBC*/pKTH11-SP_{amyE}-*nisA*; Spec^r Kan^r	This study
SC04	WB800 *thrC*::P_{xylA}-*nisBC*/pKTH11-SP_{aprE}-*nisA*; Spec^r Kan^r	This study
SC05	WB800 *thrC*::P_{xylA}-*nisBC*/pKTH11-SP_{epr}-*nisA*; Spec^r Kan^r	This study
SC06	WB800 *thrC*::P_{xylA}-*nisBC*/pKTH11-SP_{phoD}-*nisA*; Spec^r Kan^r	This study
SC07	WB800 *thrC*::P_{xylA}-*nisBC*/pKTH11-SP_{ywbN}-*nisA*; Spec^r Kan^r	This study
SC08	WB800 *thrC*::P_{xylA}-*nisBC amyE*::P_{hy_spank}-*spaT*/pKTH11-*nisA*; Spec^r Ery^r Kan^r	This study
SC09	WB800 *thrC*::P_{xylA}-*nisBC amyE*::P_{hy_spank}-*spaT*/pKTH11-S_L-*nisA*; Spec^r Ery^r Kan^r	This study
SC10	WB800 *thrC*::P_{xylA}-*nisBC amyE*::P_{hy_spank}-*spaT*/pKTH11-S_{L9}-*nisA*; Spec^r Ery^r Kan^r	This study
SC11	WB800 *thrC*::P_{xylA}-*nisBC amyE*::P_{hy_spank}-*spaT*; Spec^r Ery^r	This study
SC12	WB800 *amyE*::P_{hy_spank}-$spaT_{sfgfp}$; Ery^r	This study
SC13	WB800 *thrC*::P_{xylA}-*nisBC amyE*::P_{hy_spank}-$spaT_{sfgfp}$/pKTH11-*nisA*; Spec^r Ery^r Kan^r	This study
SC14	WB800 *thrC*::P_{xylA}-$nisB_{sfgfp}C$; Spec^r	18
SC15	WB800 *thrC*::P_{xylA}-$nisB_{sfgfp}C$ *amyE*::P_{hy_spank}-*spaT*/pKTH11-*nisA*; Spec^r Ery^r Kan^r	This study
SC16	WB800 *thrC*::P_{xylA}-$nisBC_{sfgfp}$; Spec^r	18
SC17	WB800 *thrC*::P_{xylA}-$nisBC_{sfgfp}$ *amyE*::P_{hy_spank}-*spaT*/pKTH11-*nisA*; Spec^r Ery^r Kan^r	This study
SC18	WB800 *thrC*::P_{xylA}-*nisBC amyE*::P_{hy_spank}-*spaT*/pKTH11-$nisA_{GS\text{-}His}$ ($nisA_{GS\text{-}His}$ is *nisA* extended with a factor Xa sequence, a flexible linker, and a 6×His tag); Spec^r Ery^r Kan^r	This study
SC19	NZ9000/pTLR4-*nisBTC*; Ery^r	Lab stock
SC20	NZ9000/pTLR4-*nisABC*; Ery^r	This study
SC21	NZ9000/pTLR4-*nisABTC*; Ery^r	Lab stock
SC22	NZ9000/pTLR4-*nisABC-spaT*; Ery^r	This study
SC23	NZ9000/pTLR4-*nisA-spaB-nisC-spaT*; Ery^r	This study
SC24	NZ9000/pTLR4-*nisAB-spaCT*; Ery^r	This study
SC25	NZ9000/pTLR4-*nisA-spaT*; Ery^r	This study
SC26	NZ9000/pTLR4-*spaS-nisBTC*; Ery^r	This study
SC27	NZ9000/pTLR4-*nisABC*-$spaT_{sfgfp}$; Ery^r	This study
SC28	NZ9000/pTLR4-*nisBC*-$spaT_{sfgfp}$; Ery^r	This study
SC29	NZ9000/pTLR4-*nisAB*-$spaT_{sfgfp}$; Ery^r	This study
SC30	NZ9000/pTLR4-*nisA*-$spaT_{sfgfp}$; Ery^r	This study
SC31	NZ9000/pTLR4-$spaT_{sfgfp}$; Ery^r	This study
SC32	NZ9000/pTLR4-*nisAB*-$_{mCherry}$*nisC*-$spaT_{sfgfp}$; Ery^r	This study
SC33	NZ9000/pNZE3-$spaT_{His}$/pIL3-$nisAB_{flag}C$; Ery^r Cm^r	This study
SC34	NZ9000/pNZE3-$spaT_{His}$/pIL3-$nisB_{flag}C$; Ery^r Cm^r	This study
SC35	NZ9000/pNZE3-$spaT_{His}$/pIL3-$nisB_{flag}$; Ery^r Cm^r	This study
SC36	NZ9000/pNZE3-$spaT_{His}$/pIL3-*nisC*; Ery^r Cm^r	This study
SC37	NZ9000/pNZE3-$spaT_{His}$/pIL3-*nisA*; Ery^r Cm^r	This study
SC38	NZ9000/pNZE3-$spaT_{His}$; Ery^r	This study
Plasmids		
pKTH11	*E. coli-B. subtilis* shuttle vector with P_{xylA}, a xylose-inducible promoter; Amp^r Kan^r	Lab stock
pKTH11-*nisA*	P_{xylA}-*nisA*; Amp^r Kan^r	This study
pKTH11-SP_{amyE}-*nisA*	P_{xylA}-SP_{amyE}-*nisA* (SP_{amyE} is the signal peptide); Amp^r Kan^r	This study
pKTH11-SP_{aprE}-*nisA*	P_{xylA}-SP_{aprE}-*nisA* (SP_{aprE} is the signal peptide); Amp^r Kan^r	This study
pKTH11-SP_{epr}-*nisA*	P_{xylA}-SP_{epr}-*nisA* (SP_{epr} is the signal peptide); Amp^r Kan^r	This study
pKTH11-SP_{phoD}-*nisA*	P_{xylA}-SP_{phoD}-*nisA* (SP_{phoD} is the signal peptide); Amp^r, Kan^r	This study
pKTH11-SP_{ywbN}-*nisA*	P_{xylA}-SP_{ywbN}-*nisA* (SP_{ywbN} is the signal peptide); Amp^r Kan^r	This study
pKTH11-S_L-*nisA*	P_{xylA}-S_L-*nisA* (S_L is the leader peptide of SpaS); Amp^r Kan^r	This study
pKTH11-S_{L9}-*nisA*	P_{xylA}-S_{L9}-*nisA* (S_{L9} is S_L with the N-terminal 9 residues of the core peptide of SpaS); Amp^r Kan^r	This study
pDR111	Integration vector for genomic integration into the *amyE* locus of *B. subtilis* with P_{hy_spank}, an IPTG-inducible promoter; Spec^r Amp^r	Lab stock
pDR111-*spaT*	P_{hy_spank}-*spaT*; Spec^r Amp^r	This study
pDR111-$spaT_{sfgfp}$	P_{hy_spank}-$spaT_{sfgfp}$; Spec^r Amp^r	This study

(Continued on next page)

TABLE 1 (Continued)

Strain or plasmid	Genotype and/or characteristic(s)	Reference or source
pKTH11-*nisA*$_{GS\text{-}His}$	P$_{xylA}$-*nisA*$_{GS\text{-}His}$ (*nisA*$_{GS\text{-}His}$ is *nisA* extended with a factor Xa sequence, a flexible linker, and a 6×His tag); Amp^r Kan^r	This study
pTLR4-*nisABC*	P$_{nisA}$-*nisABC*; Amp^r Ery^r	This study
pTLR4-*nisABC-spaT*	P$_{nisA}$-*nisABC-spaT*; Amp^r Ery^r	This study
pTLR4-*nisA-spaB-nisC-spaT*	P$_{nisA}$-*nisA-spaB-nisC-spaT*; Amp^r Ery^r	This study
pTLR4-*nisAB-spaCT*	P$_{nisA}$-*nisAB-spaCT*; Amp^r Ery^r	This study
pTLR4-*nisA-spaT*	P$_{nisA}$-*nisA-spaT*; Amp^r Ery^r	This study
pTLR4-*spaS-nisBTC*	P$_{nisA}$-*spaS-nisBTC*; Amp^r Ery^r	This study
pTLR4-*nisABC-spaT*$_{sfgfp}$	P$_{nisA}$-*nisABC-spaT*$_{sfgfp}$; Amp^r Ery^r	This study
pTLR4-*nisBC-spaT*$_{sfgfp}$	P$_{nisA}$-*nisBC-spaT*$_{sfgfp}$; Amp^r Ery^r	This study
pTLR4-*nisAB-spaT*$_{sfgfp}$	P$_{nisA}$-*nisAB-spaT*$_{sfgfp}$; Amp^r Ery^r	This study
pTLR4-*nisA-spaT*$_{sfgfp}$	P$_{nisA}$-*nisA-spaT*$_{sfgfp}$; Amp^r Ery^r	This study
pTLR4-*spaT*$_{sfgfp}$	P$_{nisA}$-*spaT*$_{sfgfp}$; Amp^r Ery^r	This study
pTLR4-*nisAB-*$_{mCherry}$*nisC-spaT*$_{sfgfp}$	P$_{nisA}$-*nisAB-*$_{mCherry}$*nisC-spaT*$_{sfgfp}$; Amp^r Ery^r	This study
pNZE3-*spaT*$_{His}$	P$_{nisA}$-*spaT*$_{His}$ (*spaT*$_{His}$ for 6×His-tagged SpaT); Ery^r	This study
pIL3-*nisAB*$_{flag}$*C*	P$_{nisA}$-*nisAB*$_{flag}$C (*nisB*$_{flag}$ for Flag-tagged NisB); Cm^r	This study
pIL3-*nisB*$_{flag}$*C*	P$_{nisA}$-*nisB*$_{flag}$C (*nisB*$_{flag}$ for Flag-tagged NisB); Cm^r	Lab stock
pIL3-*nisB*$_{flag}$	P$_{nisA}$-*nisB*$_{flag}$ (*nisB*$_{flag}$ for Flag-tagged NisB); Cm^r	Lab stock
pIL3-*nisC*	P$_{nisA}$-*nisC*; Cm^r	Lab stock
pIL3-*nisA*	P$_{nisA}$-*nisA*; Cm^r	Lab stock

the manufacturer's protocol. The obtained PCR products were mixed and treated with Gibson assembly master mix (Bioke, Leiden, the Netherlands), yielding 20-nucleotide overhangs annealing to complementary overhangs. The mixtures were applied to transform *E. coli* DH5α directly or *L. lactis* NZ9000 after desalting to generate plasmids. All nucleotide sequencing was performed at Macrogen Europe (Amsterdam, the Netherlands). Oligonucleotides used in this work were purchased from Biolegio BV (Nijmegen, the Netherlands) and are given in Table 2. *B. subtilis* WB800 was transformed based on natural competence (45). The transformation of *E. coli* strains was performed by heat shock according to standard procedures (44). Electrocompetent cells of *L. lactis* were transformed using electroporation with a Bio-Rad gene pulser (Bio-Rad Laboratories, Richmond, CA) (46).

Trichloroacetic acid precipitation. Trichloroacetic acid (TCA) (100%, wt/vol) was added to 45 mL of the culture supernatant at a final concentration of 10% (wt/vol) TCA. The mixture was put on ice for 2 h and then centrifuged at 10,000 × *g* for 60 min at 4°C. The pellet was retained after discarding the supernatant. Subsequently, 1/2 of the original volume of iced acetone was added to the pellet. After 60 min of centrifugation at 10,000 × *g* again, the pellet was retained and dried by vacuum freezing desiccation. Finally, the dry pellet was resuspended in 0.5 mL 50 mM Tris-HCl (pH 7.0).

Antimicrobial activity assay. *Micrococcus flavus* was used as an indicator strain and was grown overnight in GM17. One hundred microliters of the diluted culture (OD_{600} = 0.5) was added to 100 mL of melted GM17 agar at 45°C and poured onto plates. Ten-microliter samples with the addition of 1 μL purified protease NisP (laboratory stock) were dropped onto the plate after the agar was solid. The plates were left overnight at 30°C.

Mass spectrometric analysis. One microliter of each sample was spotted, dried, and washed with MilliQ water on the target. Subsequently, 1 μL of 5 mg/mL of α-cyano-4-hydroxycinnamic acid (Sigma-Aldrich) was spotted on top of the samples. An ABI Voyager DE Pro matrix-assisted laser desorption ionization–time of flight (MALDI-TOF) analyzer (Applied Biosystems) operating in linear mode using external calibration was used to obtain mass spectra.

Peptide purification. The $NisA_{GS\text{-}His}$ peptide was purified by affinity purification. *B. subtilis* cells were collected by centrifugation and washed twice with 50 mM Tris-HCl (pH 7.4). The cells were resuspended in lysis buffer (50 mM NaH_2PO_4, 300 mM NaCl, and 10 mM imidazole [pH 8.0]) with 10 mg/mL lysozyme and a protease inhibitor and incubated for 60 min at 37°C. Totals of 10 mM $MgSO_4$ and 100 mg/mL DNase I were added. After incubation for 5 min at 37°C, the suspension was passed three times through a high-pressure homogenizer (HPL6; Maximator GmbH, Germany). Two centrifugation steps at 13,000 × *g* for 10 min at 4°C were performed to remove cell debris, and the cell lysate was obtained. For Ni-NTA purification, a standard procedure was performed and conducted in a cold room (4°C). Five milliliters of lysis buffer was run over the column containing Ni-NTA agarose (50%, 1.0 mL; Qiagen Benelux BV) to equilibrate it. Subsequently, 10 mL of the lysate flowed through the column material twice to allow the 6×His-tagged peptide to bind to the Ni-NTA agarose. Next, the column material was washed twice with 10 mL wash buffer (50 mM NaH_2PO_4, 300 mM NaCl, and 20 mM imidazole [pH 8.0]). Eluates were collected in 5 fractions (0.5 mL each) using elution buffer (50 mM NaH_2PO_4, 300 mM NaCl, and 250 mM imidazole [pH 8.0]). The peptide produced by *L. lactis* was purified by C_{18} reversed-phase chromatography. *L. lactis* was grown in MEM. After centrifugation of the cultures grown overnight, the supernatants were collected, and the pH was adjusted to 7.0. After that, the supernatants were applied to

TABLE 2 Oligonucleotides used in this study

Primer	Sequence (5′→3′)
PH1	AAATCAAAGGGGGAAATCATATGAGTACAAAAGATTTTAACTTGGATTTGGTATC
PH2	GGAGGTGTTTTTTTATTACCTTATTTGCTTACGTGAATACTACAATGACAAGTTG
PH3	GGTAATAAAAAAACACCTCCAAGCTGAGTG
PH4	ATGATTTCCCCCTTTGATTTAAGTGAACAAG
PH5	AAATCAAAGGGGGAAATCATATGTTTGCAAAACGATTCAAAACCTC
PH6	TTAAAATCTTTTGTACTCATAGCACTCGCAGCCGCCGGTCCTG
PH7	ATGAGTACAAAAGATTTTAACTTGGATTTGGTATC
PH8	AAATCAAAGGGGGAAATCATATGAGAAGCAAAAAATTGTGGATCAGC
PH9	TTAAAATCTTTTGTACTCATAGCCTGCACAGACATGTTGCTG
PH10	AAATCAAAGGGGGAAATCATATGAAAAACATGTCTTGCAAACTTGTTG
PH11	TTAAAATCTTTTGTACTCATCGCATGAGCGAGAGGGCCTATG
PH12	AAATCAAAGGGGGAAATCATATGGCATACGACAGTCGTTTTGATG
PH13	TTAAAATCTTTTGTACTCATAGCATTTACTTCAAAGGCCCCAAC
PH14	AAATCAAAGGGGGAAATCATATGAGCGATGAACAGAAAAAGCCAG
PH15	TTAAAATCTTTTGTACTCATTGGCTTAGCCGCAGTCTGAAC
PH16	AAATCAAAGGGGGAAATCATATGTCAAAGTTCGATGATTTCGATTTGGATG
PH17	TTAAAATCTTTTGTACTCATTTGCGGAGTGATTTTTGAGTCTTGTTTAG
PH18	ACTCAAAAATCACTCCGCAAATGAGTACAAAAGATTTTAACTTGGATTTGG
PH19	AAATCAAAGGGGGAAATCATATGTCAAAGTTCGATGATTTCGATTTGGATG
PH20	TTAAAATCTTTTGTACTCATTGGTGTACAAAGTGATTCACTTTTCCATTG
PH21	GTGAATCACTTTGTACACCAATGAGTACAAAAGATTTTAACTTGGATTTGG
PH22	AAATCAAAGGGGGAAATCATATGGAAGTAAAGGAACAACTGAAACTAAAAG
PH23	ATGCGGCTAGCTGTCGACTATTATCTATCCTTGATACAGTGCCTCTTTCC
PH24	TAGTCGACAGCTAGCCGCATGCAAG
PH25	ATGATTTCCCCCTTTGATTTAGCTTAATTGTTATCCGCTCACAATTACAC
PH26	GTAGCGGTGGAGGTGGCAGCATGTCAAAAGGAGAAGAGCTGTTCAC
PH27	ATGCGGCTAGCTGTCGACTATTATTTACTTATAAAGCTCATCCATGCCGTG
PH28	TAGTCGACAGCTAGCCGCATGCAAG
PH29	GCTGCCACCTCCACCGCTACCTCCTTGATACAGTGCCTCTTTCCATTTAC
PH30	GGTGGAGGTGGCAGCCATCATCACCATCACCATTAATAGTCGACAGCTAGCCGCATGC
PH31	GCTGCCACCTCCACCGCTACCACGTCCTTCAATTTTGCTTACGTGAATACTACAATGAC
PH32	ATTATTCAGAGCAATATGAGGATAATGATG
PH33	ATTGCTCTGAATAATTCATTTCATGTATTCTTCCGAAACAAACAAC
PH34	CATGAAATGAGGACTAATAGATGGAAGTAAAGGAACAACTGAAACTAAAAG
PH35	TCATCAAACCTCTGAATTCCTTATCCTTGATACAGTGCCTCTTTCCATTTAC
PH36	GGAATTCAGAGGTTTGATGACTTTGACC
PH37	CTATTAGTCCTCATTTCATGTCATTTCCTCTTCCCTCCTTTCAAAAAATCG
PH38	AAATAAAGAGAGGAAAAAACATGAAATCCTTATATACACCTACAGATTATTATATGATTC
PH39	CATATTGCTCTGAATAATTTACTTCCATGCTAAACTACCATTCATCTTTTG
PH40	TAAATTATTCAGAGCAATATGAGGATAATGATG
PH41	GTTTTTTCCTCTCTTTATTTTTATAAGCTATTTAGCAACC
PH42	AATTATTCAGAGCAATATGGAAAGAGGCACTGTATCAAGGATAG
PH43	CTATTAGTCCTCATTTCATGTTAAATTAATAATGCTTTTGTCCAATCTGTTTTTGAG
PH44	CATGAAATGAGGACTAATAGATGGAAGTAAAGGAACAACTGAAACTAAAAG
PH45	CCATATTGCTCTGAATAATTCATTTCATGTATTCTTCC
PH46	CATGAAATGAGGACTAATAGATGGAAGTAAAGGAACAACTGAAACTAAAAG
PH47	TAGTCCTCATTTCATGTATTTTTATAAGCTATTTAGCAACCCTAAATAACTTATAAAAATAGG
PH48	ATTATAAGGAGGCACTCAAAATGTCAAAGTTCGATGATTTCGATTTGG
PH49	AATACTATCCTTTGATTTGGTTATTTAGAGATTTTGCAGTTACAAGTTAGTGTTTG
PH50	CCAAATCAAAGGATAGTATTTTGTTAGTTCAGAC
PH51	TTTGAGTGCCTCCTTATAATTTATTTTGTAGTTCC
PH52	GTAGCGGTGGAGGTGGCAGCATGTCAAAAGGAGAAGAGCTGTTCAC
PH53	TCATCAAACCTCTGAATTCCTTACTTATAAAGCTCATCCATGCCGTG
PH54	GCTGCCACCTCCACCGCTACCTCCTTGATACAGTGCCTCTTTCCATTTAC
PH55	CCAAATCAAAGGATAGTATTTTGTTAGTTCAGAC
PH56	TATCCTTTGATTTGGTTTGAGTGCCTCCTTATAATTTATTTTGTAGTTCC
PH57	CATGAAATGAGGACTAATAGATGGAAGTAAAGGAACAACTGAAACTAAAAG
PH58	CTATTAGTCCTCATTTCATGTATTCTTCCGAAAC
PH59	CATGAAATGAGGACTAATAGATGGAAGTAAAGGAACAACTGAAACTAAAAG
PH60	CTATTAGTCCTCATTTCATGTATTTTTATAAGCTATTTAGC
PH61	ATGAGCAAAGGAGAAGAAGATAACATGG
PH62	GCTGCCACCTCCACCGCTACCTTTGTAAAGCTCATCCATTCCGCCAGTTG

(Continued on next page)

TABLE 2 (Continued)

Primer	Sequence (5′→3′)
PH63	GTAGCGGTGGAGGTGGCAGCAGGATAATGATGAATAAAAAAAATATAAAAAGAAATGTTG
PH64	TCTTCTTCTCCTTTGCTCATATTGCTCTGAATAATTCATTTCATGTATTCTTCC
PH65	ATGGAAGTAAAGGAACAACTGAAACTAAAAGAG
PH66	TGATGGTGATGGTGATGATGTCCTTGATACAGTGCCTCTTTCCATTTAC
PH67	CATCATCACCATCACCATCATCACTAAGGATCCGCTTTCTTTGAACCAAAATTAG
PH68	AGTTGTTCCTTTACTTCCATTTTGAGTGCCTCCTTATAATTTATTTTGTAGTTCC
PH69	CATGACATTGACTATAAAGACGATGACGATAAATGAATTATTCAGAGCAATATGAGGATAATGATG
PH70	ATCTTTATAGTCTCCGTCATGATCTTTATAGTCTTTCATGTATTCTTCCGAAACAAACAACC

Sigma-Aldrich C_{18} silica gel spherically equilibrated with 10 column volumes (CVs) of 100% aqueous acetonitrile (MeCN) containing 0.1% trifluoroacetic acid. After washing with 10 CVs of MilliQ water with 0.1% trifluoroacetic acid, the peptide was eluted from the column using 10 CVs of ~30 to 60% aqueous MeCN containing 0.1% trifluoroacetic acid. Fractions containing the eluted peptide were freeze-dried. Finally, the peptide was dissolved in MilliQ water containing 0.1% trifluoroacetic acid.

Membrane protein purification. *L. lactis* cells were collected by centrifugation and washed twice with 50 mM Tris-HCl (pH 7.4). The harvested cells were resuspended in lysis buffer (50 mM Tris-HCl and 300 mM KCl [pH 7.4]) with 10 mg/mL lysozyme and a protease inhibitor and incubated for 60 min at 37°C. Totals of 10 mM $MgSO_4$ and 100 mg/mL DNase I were added. After incubation for 5 min at 37°C, the suspension was passed three times through a high-pressure homogenizer (HPL6; Maximator GmbH, Germany). Membrane fractions were obtained by ultracentrifugation and resuspended in binding buffer (50 mM Tris-HCl, 300 mM NaCl, and 10 mM imidazole [pH 7.4]). The total membrane protein concentration was measured by a bicinchoninic acid (BCA) assay (Thermo Fisher Scientific). Membranes were solubilized with 1% (wt/vol) *n*-dodecyl-β-D-maltoside (DDM) for 2 h at 4°C. Insoluble material was removed by ultracentrifugation at 40,000 $\times$ *g* for 30 min. Ten milliliters of binding buffer with 0.1% (wt/vol) DDM was run over the column containing Ni-NTA agarose (50%, 1.0 mL; Qiagen Benelux BV) to equilibrate it. Subsequently, 10 mL of the soluble membrane was mixed with 0.5 mL of Ni-NTA agarose and incubated at 4°C for 2 h with shaking to allow the 6×His-tagged protein to bind to the Ni-NTA agarose. The soluble membrane flowed through the column material. Next, the column material was washed twice with 10 mL wash buffer (50 mM Tris-HCl, 300 mM NaCl, 20 mM imidazole, and 0.1% [wt/vol] DDM [pH 7.4]). Eluates were collected in 5 fractions (0.5 mL each) using elution buffer (50 mM Tris-HCl, 300 mM NaCl, 300 mM imidazole, and 0.1% [wt/vol] DDM [pH 7.4]). Finally, purified proteins were analyzed by SDS-PAGE and Western blotting.

SDS-PAGE and Western blotting. The samples for glycine or Tricine SDS-PAGE were incubated in loading buffer containing 5% (vol/vol) β-mercaptoethanol and boiled for 10 min. SDS-PAGE was performed according to a standard operation manual (44). Western blot assays were performed using anti-His, antileader, anti-Flag, and anti-NisC antibodies.

Fluorescence microscopy. All micrographs were captured using a DeltaVision Elite inverted epifluorescence microscope (Applied Precision, GE Healthcare, Issaquah, WA, USA) equipped with a stage holder, a climate chamber, a seven-color combined-set InsightSSI solid-state illumination module, and a scientific complementary metal oxide semiconductor (sCMOS) camera (PCO AG, Kelheim, Germany). A 100× phase-contrast objective (numerical aperture [NA], 1.4; oil immersion [Deltavision; Olympus, Japan]) was used for image capturing, in combination with SoftWorX 3.6.0 software (Applied Precision) to control the microscope setup. Standard fluorescence filter sets were used to visualize sfGFP, with excitation at 475/28 nm and emission at 525/48 nm, and mCherry, with excitation at 573.5/33 nm and emission at 607.5/19 nm. A standard microscope slide was prepared with a layer of solidified agarose (1% [wt/vol] in the appropriate medium), and 1 μL of bacterial cells was loaded onto the agarose. The sample was covered with a standard microscope coverslip for microscopic observations.

Data analysis of microscopy images. Images were deconvoluted with SoftWorks imaging software. Color assignment and overlay images were created using ImageJ software (https://imagej.net/Fiji) and saved as green/red tagged-image file format (TIFF) files. ImageJ-based ScatterJ was employed to determine Pearson's correlation coefficient (PCC) (47). Prior to ScatterJ analysis, the images were processed with a discoidal averaging filter to increase the signal-to-noise ratio of the detected foci and remove all background signals. The PCC is a well-established measure of correlation and has a range from +1 (perfect correlation) to −1 (perfect but negative correlation), with 0 denoting the absence of a relationship. All different images were acquired with the same exposure time. Image processing consists of equivalent adjustments of brightness and contrast on complete images. Gamma and LUT (lookup table) values were not modified and were left as linear on each channel. In this study, all the experiments were repeated at least 3 times.

SUPPLEMENTAL MATERIAL

Supplemental material is available online only.

SUPPLEMENTAL FILE 1, PDF file, 0.8 MB.

ACKNOWLEDGMENTS

J.C. was financially supported by the China Scholarship Council (CSC) (no. 201604910574).

O.P.K. and J.C. conceived the project and strategy. O.P.K. supervised the work and corrected the manuscript. J.C. designed and carried out the experiments, analyzed data, and wrote the manuscript. Both authors contributed to and commented on the manuscript text and approved its final version.

REFERENCES

1. Arnison PG, Bibb MJ, Bierbaum G, Bowers AA, Bugni TS, Bulaj G, Camarero JA, Campopiano DJ, Challis GL, Clardy J, Cotter PD, Craik DJ, Dawson M, Dittmann E, Donadio S, Dorrestein PC, Entian K-D, Fischbach MA, Garavelli JS, Goransson U, Gruber CW, Haft DH, Hemscheidt TK, Hertweck C, Hill C, Horswill AR, Jaspars M, Kelly WL, Klinman JP, Kuipers OP, Link AJ, Liu W, Marahiel MA, Mitchell DA, Moll GN, Moore BS, Muller R, Nair SK, Nes IF, Norris GE, Olivera BM, Onaka H, Patchett ML, Piel J, Reaney MJT, Rebuffat S, Ross RP, Sahl H-G, Schmidt EW, Selsted ME, et al. 2013. Ribosomally synthesized and post-translationally modified peptide natural products: overview and recommendations for a universal nomenclature. Nat Prod Rep 30:108–160. https://doi.org/10.1039/c2np20085f.
2. Montalban-Lopez M, Scott TA, Ramesh S, Rahman IR, van Heel AJ, Viel JH, Bandarian V, Dittmann E, Genilloud O, Goto Y, Grande Burgos MJ, Hill C, Kim S, Koehnke J, Latham JA, Link AJ, Martinez B, Nair SK, Nicolet Y, Rebuffat S, Sahl H-G, Sareen D, Schmidt EW, Schmitt L, Severinov K, Sussmuth RD, Truman AW, Wang H, Weng J-K, van Wezel GP, Zhang Q, Zhong J, Piel J, Mitchell DA, Kuipers OP, van der Donk WA. 2021. New developments in RiPP discovery, enzymology and engineering. Nat Prod Rep 38:130–239. https://doi.org/10.1039/d0np00027b.
3. Lubelski J, Rink R, Khusainov R, Moll GN, Kuipers OP. 2008. Biosynthesis, immunity, regulation, mode of action and engineering of the model lantibiotic nisin. Cell Mol Life Sci 65:455–476. https://doi.org/10.1007/s00018-007-7171-2.
4. de Ruyter PG, Kuipers OP, Beerthuyzen MM, van Alen-Boerrigter I, de Vos WM. 1996. Functional analysis of promoters in the nisin gene cluster of *Lactococcus lactis*. J Bacteriol 178:3434–3439. https://doi.org/10.1128/jb.178.12.3434-3439.1996.
5. Stein T, Borchert S, Kiesau P, Heinzmann S, Kloss S, Klein C, Helfrich M, Entian KD. 2002. Dual control of subtilin biosynthesis and immunity in *Bacillus subtilis*. Mol Microbiol 44:403–416. https://doi.org/10.1046/j.1365-2958.2002.02869.x.
6. Kaletta C, Entian KD. 1989. Nisin, a peptide antibiotic: cloning and sequencing of the *nisA* gene and posttranslational processing of its peptide product. J Bacteriol 171:1597–1601. https://doi.org/10.1128/jb.171.3.1597-1601.1989.
7. Khusainov R, Moll GN, Kuipers OP. 2013. Identification of distinct nisin leader peptide regions that determine interactions with the modification enzymes NisB and NisC. FEBS Open Bio 3:237–242. https://doi.org/10.1016/j.fob.2013.05.001.
8. Kuipers A, de Boef E, Rink R, Fekken S, Kluskens LD, Driessen AJM, Leenhouts K, Kuipers OP, Moll GN. 2004. NisT, the transporter of the lantibiotic nisin, can transport fully modified, dehydrated, and unmodified prenisin and fusions of the leader peptide with non-lantibiotic peptides. J Biol Chem 279:22176–22182. https://doi.org/10.1074/jbc.M312789200.
9. Ge X, Teng K, Wang J, Zhao F, Zhang J, Zhong J. 2017. Identification of key residues in the NisK sensor region for nisin biosynthesis regulation. Front Microbiol 8:106. https://doi.org/10.3389/fmicb.2017.00106.
10. Alkhatib Z, Abts A, Mavaro A, Schmitt L, Smits SHJ. 2012. Lantibiotics: how do producers become self-protected? J Biotechnol 159:145–154. https://doi.org/10.1016/j.jbiotec.2012.01.032.
11. Montalban-Lopez M, Deng JJ, van Heel AJ, Kuipers OP. 2018. Specificity and application of the lantibiotic protease NisP. Front Microbiol 9:160. https://doi.org/10.3389/fmicb.2018.00160.
12. Lagedroste M, Smits SHJ, Schmitt L. 2017. Substrate specificity of the secreted nisin leader peptidase NisP. Biochemistry 56:4005–4014. https://doi.org/10.1021/acs.biochem.7b00524.
13. Siegers K, Heinzmann S, Entian KD. 1996. Biosynthesis of lantibiotic nisin. Posttranslational modification of its prepeptide occurs at a multimeric membrane-associated lanthionine synthetase complex. J Biol Chem 271:12294–12301. https://doi.org/10.1074/jbc.271.21.12294.
14. Kiesau P, Eikmanns U, Gutowski-Eckel Z, Weber S, Hammelmann M, Entian KD. 1997. Evidence for a multimeric subtilin synthetase complex. J Bacteriol 179:1475–1481. https://doi.org/10.1128/jb.179.5.1475-1481.1997.
15. Khusainov R, Heils R, Lubelski J, Moll GN, Kuipers OP. 2011. Determining sites of interaction between prenisin and its modification enzymes NisB and NisC. Mol Microbiol 82:706–718. https://doi.org/10.1111/j.1365-2958.2011.07846.x.
16. Reiners J, Abts A, Clemens R, Smits SHJ, Schmitt L. 2017. Stoichiometry and structure of a lantibiotic maturation complex. Sci Rep 7:42163. https://doi.org/10.1038/srep42163.
17. Chen J, van Heel AJ, Kuipers OP. 2020. Subcellular localization and assembly process of the nisin biosynthesis machinery in *Lactococcus lactis*. mBio 11:e02825-20. https://doi.org/10.1128/mBio.02825-20.
18. Chen J, van Heel AJ, Kuipers OP. 2021. Visualization and analysis of the dynamic assembly of a heterologous lantibiotic biosynthesis complex in *Bacillus subtilis*. mBio 12:e01219-21. https://doi.org/10.1128/mBio.01219-21.
19. Chen J, Kuipers OP. 2021. Isolation and analysis of the nisin biosynthesis complex NisBTC: further insights into their cooperative action. mBio 12:e02585-21. https://doi.org/10.1128/mBio.02585-21.
20. Lagedroste M, Reiners J, Smits SHJ, Schmitt L. 2020. Impact of the nisin modification machinery on the transport kinetics of NisT. Sci Rep 10:12295. https://doi.org/10.1038/s41598-020-69225-2.
21. Garg N, Salazar-Ocampo LMA, van der Donk WA. 2013. In vitro activity of the nisin dehydratase NisB. Proc Natl Acad Sci U S A 110:7258–7263. https://doi.org/10.1073/pnas.1222488110.
22. Li B, Yu JPJ, Brunzelle JS, Moll GN, van der Donk WA, Nair SK. 2006. Structure and mechanism of the lantibiotic cyclase involved in nisin biosynthesis. Science 311:1464–1467. https://doi.org/10.1126/science.1121422.
23. Kuipers OP, Rollema HS, de Vos WM, Siezen RJ. 1993. Biosynthesis and secretion of a precursor of nisin Z by *Lactococcus lactis*, directed by the leader peptide of the homologous lantibiotic subtilin from *Bacillus subtilis*. FEBS Lett 330:23–27. https://doi.org/10.1016/0014-5793(93)80911-d.
24. Chakicherla A, Hansen JN. 1995. Role of the leader and structural regions of prelantibiotic peptides as assessed by expressing nisin-subtilin chimeras in *Bacillus subtilis* 168, and characterization of their physical, chemical, and antimicrobial properties. J Biol Chem 270:23533–23539. https://doi.org/10.1074/jbc.270.40.23533.
25. Spieß T, Korn SM, Kötter P, Entian K-D. 2015. Autoinduction specificities of the lantibiotics subtilin and nisin. Appl Environ Microbiol 81:7914–7923. https://doi.org/10.1128/AEM.02392-15.
26. Geiger C, Spieß T, Korn SM, Kötter P, Entian K-D. 2017. Specificity of subtilin-mediated activation of histidine kinase SpaK. Appl Environ Microbiol 83:e00781-17. https://doi.org/10.1128/AEM.00781-17.
27. Stein T, Heinzmann S, Solovieva I, Entian KD. 2003. Function of *Lactococcus lactis* nisin immunity genes *nisI* and *nisFEG* after coordinated expression in the surrogate host *Bacillus subtilis*. J Biol Chem 278:89–94. https://doi.org/10.1074/jbc.M207237200.
28. Hacker C, Christ NA, Duchardt-Ferner E, Korn S, Gobl C, Berninger L, Dusterhus S, Hellmich UA, Madl T, Kotter P, Entian KD, Wohnert J. 2015. The solution structure of the lantibiotic immunity protein NisI and its interactions with nisin. J Biol Chem 290:28869–28886. https://doi.org/10.1074/jbc.M115.679969.
29. van Tilburg AY, van Heel AJ, Stulke J, de Kok NAW, Rueff AS, Kuipers OP. 2020. Mini*Bacillus* PG10 as a convenient and effective production host for lantibiotics. ACS Synth Biol 9:1833–1842. https://doi.org/10.1021/acssynbio.0c00194.
30. Kuipers A, Wierenga J, Rink R, Kluskens LD, Driessen AJM, Kuipers OP, Moll GN. 2006. Sec-mediated transport of posttranslationally dehydrated peptides in *Lactococcus lactis*. Appl Environ Microbiol 72:7626–7633. https://doi.org/10.1128/AEM.01802-06.

31. Kuipers A, Rink R, Moll GN. 2009. Translocation of a thioether-bridged azurin peptide fragment via the Sec pathway in *Lactococcus lactis*. Appl Environ Microbiol 75:3800–3802. https://doi.org/10.1128/AEM.00341-09.
32. Caspers M, Brockmeier U, Degering C, Eggert T, Freudl R. 2010. Improvement of Sec-dependent secretion of a heterologous model protein in *Bacillus subtilis* by saturation mutagenesis of the N-domain of the AmyE signal peptide. Appl Microbiol Biotechnol 86:1877–1885. https://doi.org/10.1007/s00253-009-2405-x.
33. Chen JQ, Gai YM, Fu G, Zhou WJ, Zhang DW, Wen JP. 2015. Enhanced extracellular production of α-amylase in *Bacillus subtilis* by optimization of regulatory elements and over-expression of PrsA lipoprotein. Biotechnol Lett 37:899–906. https://doi.org/10.1007/s10529-014-1755-3.
34. Cui WJ, Suo FY, Cheng JT, Han LC, Hao WL, Guo JL, Zhou ZM. 2018. Stepwise modifications of genetic parts reinforce the secretory production of nattokinase in *Bacillus subtilis*. Microb Biotechnol 11:930–942. https://doi.org/10.1111/1751-7915.13298.
35. Ren GH, Cao LC, Kong W, Wang ZJ, Liu YH. 2016. Efficient secretion of the β-galactosidase Bgal1-3 via both Tat-dependent and Tat-independent pathways in *Bacillus subtilis*. J Agric Food Chem 64:5708–5716. https://doi.org/10.1021/acs.jafc.6b01735.
36. Liu RH, Zuo ZQ, Xu YM, Song CJ, Jiang H, Qiao CL, Xu P, Zhou QX, Yang C. 2014. Twin-arginine signal peptide of *Bacillus subtilis* YwbN can direct Tat-dependent secretion of methyl parathion hydrolase. J Agric Food Chem 62:2913–2918. https://doi.org/10.1021/jf405694n.
37. Corvey C, Stein T, Dusterhus S, Karas M, Entian KD. 2003. Activation of subtilin precursors by *Bacillus subtilis* extracellular serine proteases subtilisin (AprE), WprA, and Vpr. Biochem Biophys Res Commun 304:48–54. https://doi.org/10.1016/s0006-291x(03)00529-1.
38. Lagedroste M, Smits SHJ, Schmitt L. 2021. Importance of the leader peptide sequence on the lanthipeptide secretion level. FEBS J 288:4348–4363. https://doi.org/10.1111/febs.15724.
39. van Saparoea HBV, Bakkes PJ, Moll GN, Driessen AJM. 2008. Distinct contributions of the nisin biosynthesis enzymes NisB and NisC and transporter NisT to prenisin production by *Lactococcus lactis*. Appl Environ Microbiol 74:5541–5548. https://doi.org/10.1128/AEM.00342-08.
40. de Ruyter PG, Kuipers OP, de Vos WM. 1996. Controlled gene expression systems for *Lactococcus lactis* with the food-grade inducer nisin. Appl Environ Microbiol 62:3662–3667. https://doi.org/10.1128/aem.62.10.3662-3667.1996.
41. Engelke G, Gutowski-Eckel Z, Hammelmann M, Entian KD. 1992. Biosynthesis of the lantibiotic nisin: genomic organization and membrane localization of the NisB protein. Appl Environ Microbiol 58:3730–3743. https://doi.org/10.1128/aem.58.11.3730-3743.1992.
42. Plat A, Kluskens LD, Kuipers A, Rink R, Moll GN. 2011. Requirements of the engineered leader peptide of nisin for inducing modification, export, and cleavage. Appl Environ Microbiol 77:604–611. https://doi.org/10.1128/AEM.01503-10.
43. Mavaro A, Abts A, Bakkes PJ, Moll GN, Driessen AJM, Smits SHJ, Schmitt L. 2011. Substrate recognition and specificity of the NisB protein, the lantibiotic dehydratase involved in nisin biosynthesis. J Biol Chem 286:30552–30560. https://doi.org/10.1074/jbc.M111.263210.
44. Sambrook J, Russell DW. 2001. Molecular cloning: a laboratory manual, 3rd ed. Cold Spring Harbor Laboratory Press, Cold Spring Harbor, NY.
45. Harwood CR, Cutting SM. 1990. Molecular biological methods for Bacillus. John Wiley & Sons, Chichester, United Kingdom.
46. Holo H, Nes IF. 1989. High-frequency transformation, by electroporation, of *Lactococcus lactis* subsp. *cremoris* grown with glycine in osmotically stabilized media. Appl Environ Microbiol 55:3119–3123. https://doi.org/10.1128/aem.55.12.3119-3123.1989.
47. Zeitvogel F, Schmid G, Hao L, Ingino P, Obst M. 2016. ScatterJ: an ImageJ plugin for the evaluation of analytical microscopy datasets. J Microsc 261:148–156. https://doi.org/10.1111/jmi.12187.
48. Kuipers OP, Beerthuyzen MM, Siezen RJ, De Vos WM. 1993. Characterization of the nisin gene cluster *nisABTCIPR* of *Lactococcus lactis*. Requirement of expression of the *nisA* and *nisI* genes for development of immunity. Eur J Biochem 216:281–291. https://doi.org/10.1111/j.1432-1033.1993.tb18143.x.
49. Zhang XZ, Cui ZL, Hong Q, Li SP. 2005. High-level expression and secretion of methyl parathion hydrolase in *Bacillus subtilis* WB800. Appl Environ Microbiol 71:4101–4103. https://doi.org/10.1128/AEM.71.7.4101-4103.2005.